



Technical Sciences  
Academy of Romania  
[www.jesi.astr.ro](http://www.jesi.astr.ro)

## Journal of Engineering Sciences and Innovation

Volume 9, Issue 4 / 2024, p. 449-458

<http://doi.org.10.56958/jesi.2024.9.4.449>

**F. Electrical, Electronics Engineering,  
Computer Sciences and Engineering**

Received 20 August 2024

Accepted 4 December 2024

Received in revised form 13 October 2024

### Modeling and control for a maglev system using Simulink platform simulation

AVIJIT MALLIK<sup>1,\*</sup>, RAHAT RAHMAN<sup>1</sup>, SHAISFUL ISLAM<sup>2</sup>

<sup>1</sup>Dept. of Mechanical Engineering, RUET, Rajshahi-6204, Bangladesh

<sup>2</sup>Dept. of Electrical & Electronic Engineering, RUET, Rajshahi-6204, Bangladesh

**Abstract.** Magnetic Levitation is very popular now a days because of the base grating and low energy utilization which views as significant issues. This paper proposed an PID control for magnetic levitation system utilizing continuous control Simulink highlight of (SIMLAB) microcontroller. The control arrangement of the maglev transportation framework is checked by recreations with test results, and its prevalence is shown in correlation with past writing and traditional control procedures. Likewise, the proposed framework was executed under impact of relative essential subordinate controller/PID. Too, the controller framework execution was thought about in term of three parameters Peak overshoot, Settling time and Rise time. The discoveries demonstrate the understanding of recreation with exploratory outcomes got. In addition, the controller delivered an extraordinary soundness and homogeneous reaction than different controllers utilized. For trial results, the PID brought a 14.6%, 0.199 and 0.064 for top overshoot, Setting time and Rise time individually.

**Keywords:** Maglev, Magnetic Control, Magnetism, PID.

#### 1. Introduction

Magnetic levitation (maglev) or suspension is a system by which a ferromagnetic object is suspended with no help other than magnetic fields. Magnetic power is utilized to check the impacts of the gravitational acceleration and some other increasing speeds. The two essential issues associated with magnetic levitation are lifting powers: giving an upward power adequate to balance gravity, and strength which guarantees the stability of the system not being precipitously slide or flipped into an arrangement where the lift is neutralized. Magnetic levitation is utilized for maglev trains, contactless liquefying, attractive orientation and for item show

---

\*Correspondence address: [avijitme13@gmail.com](mailto:avijitme13@gmail.com)

purposes. For fruitful levitation and control of each of the 6 axes (degrees of freedom; 3 translational and 3 rotational) a mix of lasting magnets and electromagnets or diamagnets or superconductors just as alluring and terrible fields can be utilized. From Earnshaw's hypothesis in any event one stable pivot must be available for the framework to suspend effectively, however different DoF (Degrees of Freedom) can be settled utilizing ferromagnetism.

Magnetic levitation is an ideal answer to accomplish better execution for some dynamic frameworks, e.g., exact positioning, control, suspension, and haptic communication because of its non-contact, non-tainting, multi-Degrees-Of-Freedom (DOF), and long-stroke attributes. One of the highlights of maglev frameworks is decrease of creative mind, which makes them pleasant in the field of genuine applications [1], which are transportation frameworks [2], air stream levitation [3], attractive bearing frameworks and against vibration table [4]. These systems are intrinsically nonlinear and insecure too. Along these lines, the maglev framework is likewise a fascinating issue to affirm the presentation of control plans. Be that as it may, numerous strategies were utilized to control these frameworks [5].

Yaghoubi and Georgios (2019) [6] had worked on a feed forward multilayer neural system was utilized to display the framework, in which learning, and control is done at the same time. Just as certain works were done dependent on neural systems. Dynamic neural systems for the example acknowledgment are planned and actualized in [7]. Likewise, effective systems of versatile controllers are examined in Suganthan & Rakesh (2021) along with Frankel et al. 2021 [8, 9]. Zhou et al. 2022 [10], had worked on stable neural controllers of nonlinear frameworks and in that research the ways of neural controller unit behaviors are structured. In Chhilar & Ankur (2020) [11], new iterative versatile powerful programming based ideal controllers are proposed and tried. Different strategies for PI controller are plan and have been tried [12–16]. Be that as it may, the attractive levitation framework has shaky nonlinear elements which ought to be taken in tally. A large portion of the commitments require estimations of position, speed and electric flow, and consequently state onlookers ought to be orchestrated to assess the inaccessible signs of the nonlinear dynamical framework. Moreover, it needs to plan complex frameworks and a portion of these frameworks are expensive. Considering the notice study, a controller to balance out this framework ought to be of extraordinary intrigue. In this examination, a model and a controller are acquainted for a functioning strategy with control the maglev framework dependent on SIMULINK stage. The maglev framework utilized was confirmed hypothetically and with reproductions also. The control frameworks were thought about under different parameters. The discoveries indicated an understanding for both reproduction and past exploratory outcomes.

## 2. Problem Formulation

For any successive simulation, it needs to be theoretically modelled with as much complexity as possible. The system is made up of electromagnets as actuators for applying magnetic forces to achieve stable levitation and precise position control, a rigid square plate with permanent magnets on corner, and Hall effect sensors for sensing the position of the levitating plate.  $V_a$  is the coil applied voltage. The electromagnets are 15 mH solenoid coils with 2 X internal resistances. The Hall Effect sensors are linear radiometric Hall Effect sensors with 50 V/T. The permanent magnets are N52 neodymium disc magnets with 12.70 mm diameter and 6.35 mm thickness. The plate is a transparent one having volume of 152.4 mm × 152.4 mm × 3.175 mm. The frame is taken as an insulator media. The model of the system is shown in Fig. 1, where  $R$  is the resistance of the coil,  $L$  is the inductance of the coil,  $v$  is the voltage across the electromagnet,  $i$  is the current through the electromagnet,  $m$  is the mass of the levitating magnet,  $g$  is the acceleration due to gravity,  $d$  is the vertical position of the levitating magnet measured from the bottom of the electromagnet,  $f$  is the force on the levitating magnet generated by the electromagnet and  $e$  is the voltage across the Hall effect sensor.

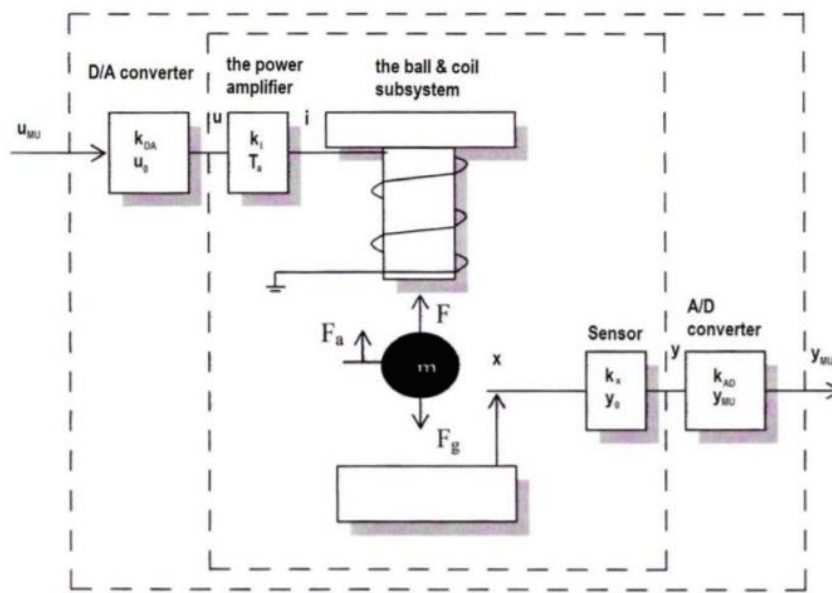


Fig. 1. Magnetic levitation.

In this section, the mathematical model of maglev system has been presented. The force actuated by the electromagnet is formulated as [21]:

$$F_{magnetic} = C \frac{i(t)}{d^3}, \tag{1}$$

where  $i(t)$  denotes the current across the electromagnet,  $d$  is the vertical position and  $C$  is a constant related to turn ratio and cross-sectional area of the electromagnet. From a force balancing equation, we have,

$$M\ddot{d} = mg - C \frac{i(t)}{d^3}, \tag{2}$$

where  $m$  is the mass of the levitating magnet plus one-fourth of the mass of the acrylic plate and  $g$  is the acceleration due to gravity. In addition, an electrical relation of the voltage supply and the electromagnetic coil can be expressed by,

$$v(t) = R \cdot i(t) + L \frac{di}{dt} \tag{3}$$

where  $R$  and  $L$  are resistance and inductance of the electromagnet, respectively. Now consider the following perturbations with respect to the change of them,

$$\begin{cases} v(t) = v_0 + \Delta v(t) \\ d(t) = d_0 + \Delta d(t) \\ i(t) = i_0 + \Delta i(t) \end{cases} \tag{4}$$

Table. 1. Proposed System Parameters

Variable Name	Symbol of representation	Value	Unit
Sensor	$\beta$	$5.64 \times 10^{-4}$	V.m <sup>2</sup>
	$\gamma$	0.31	V/A
	$\alpha$	2.48	V
Operation Point	$I_0$	1	A
	$D_0$	20	Mm
Electromagnet	$C$	$2.4 \times 10^{-6}$	Kg.m <sup>5</sup> /s <sup>2</sup> A
	$R$	2	$\Omega$
	$L$	$10 \times 10^{-3}$	H
	$m = M/4$	0.01875	Kg

where  $v_0$  is the required equilibrium coil voltage to suspend the levitating plate at  $d_0$ . Under this perturbation, the dynamics (2) and (3) around an operating point ( $i_0; d_0; v_0$ ) can be linearized as

$$m\ddot{\Delta d} = \left( \frac{3Ci_0}{d_0^4} \right) \Delta d - (C/d_0^3) \Delta i \tag{5}$$

$$\dot{\Delta i} = -\left( \frac{R\Delta i}{L} \right) - \Delta v/L \tag{6}$$

where  $\Delta i, \Delta v, \Delta d$  is linearization of the system about the equilibrium point. After eliminating  $\Delta i$  in (6) and applying Laplace transforms, we obtain the transfer function from  $\Delta v$  to  $\Delta d$  given as

$$\frac{\Delta D(s)}{\Delta V(s)} = \frac{-gR/v_0}{(Ls+R)(s^2 - \frac{3Ci_0}{md_0^4})} \tag{7}$$

where  $\Delta V(s)$  and  $\Delta D(s)$  denote the Laplace transforms of  $\Delta v(t)$  and  $\Delta d(t)$ , respectively. Hall sensor has an output voltage of the given form [22]

$$e(t) = \alpha + \frac{\beta}{a^2} + \gamma i(t) \tag{8}$$

where  $a, b, c$  are constant sensor parameters. A linearization of (8) around  $e(t) = e_0 + \Delta e$  results in

$$\Delta e = \frac{-2\beta\Delta d}{d_0^3} + \gamma\Delta i \quad (9)$$

where  $\Delta e$  is the sensor voltage. Applying Laplace transform to (9) and using  $I(s) = \Delta V(s)/(Ls + R)$  from (3) and the representation in (7), we obtain a relation between the electromagnet voltage  $\Delta V(s)$  and a sensor voltage perturbation  $\Delta E(s)$  as follows;

$$\frac{\Delta E(s)}{\Delta V(s)} = \frac{\gamma(s^2 - \frac{3ci}{md_0^4}) + \frac{2\beta RC}{md_0^6}}{(Ls+R)(s^2 - 3ci/md_0^4)} \quad (10)$$

Eq. (10) can represent also in the state space form after applying the second derivative of (5) and first derivative of (6). Thus, the state space representation of the linearized model of Eq. (10) can be represented by followings:

$$\begin{bmatrix} \dot{x}_1 \\ \dot{x}_2 \\ \dot{x}_3 \end{bmatrix} = \begin{bmatrix} 0 & 1 & 0 \\ 3\frac{ci_0}{md_0^4} & 0 & -\frac{c}{md_0^3} \\ 0 & 0 & -R/L \end{bmatrix} + \begin{bmatrix} 0 \\ 0 \\ 1/L \end{bmatrix}. \quad (11)$$

The measured output system ( $y$ ) can be obtained after simplified Eq. (9), where ( $\Delta e = y$ ,  $\Delta d = x_1$ , and  $\Delta i = x_3$ )

$$y = \begin{bmatrix} \frac{-2\beta}{d^3} & 0 & \gamma \end{bmatrix} \begin{bmatrix} x_1 \\ x_2 \\ x_3 \end{bmatrix}. \quad (12)$$

Suppose that  $x = [x_1 \ x_2 \ x_3] = [d \ \dot{d} \ i]$  is the state of the system, where  $d$  is the controlled output,  $y = e$  is the measured output and  $u = v$  is the control input by substituting system parameters in Table 1 into (10),

$$G(s).H(s) = \frac{20.66s^2 + 61803}{s^3 + 132.5s^2 - 1470s - 194900} \quad (13)$$

As the levitating object is controlled by current, which comes directly from amplifier and thus by design it is constant. So, the power can be described by following transfer function, where the variable gap can be labeled as;

$$\frac{I(s)}{U(s)} = \frac{K_i}{T_a s + 1}, \quad (14)$$

where,  $T_a$  = Coil amplified time constant;  $K_i$  = Coil amplified gain;  $I(s)$  = Output Current;  $U(s)$  = Input Voltage.

### 3. PID controller

The schematic diagram of PID controller is given in Fig. 2. This control system is working based on the calculations of the error value, trying to reduce the error percentage by adjusting the controller parameters. The general form of this controller formulated as in below [18]:

$$u(t) = K_p(e(t) + \frac{1}{T_i} \int_0^t e(\tau) d\tau + T_d \frac{de(t)}{dt}) \quad (15)$$

where:  $u(t)$ : denote the control signal  $K_p$ : the proportional gain,  $T_i$ : integral time  $T_d$ : derivative time,  $K_p$ ,  $T_i$ ,  $T_d$ : the control parameters for tuning and  $e(t)$ : the difference between the reference point and actual plant. By placing the closed loop poles at  $P = [132.45 \ 38.36 - 28.36]$ , the PID gains calculated are [ $K_p = 10$ ,  $K_i = 4$ ,  $K_D = 0.2$ ].

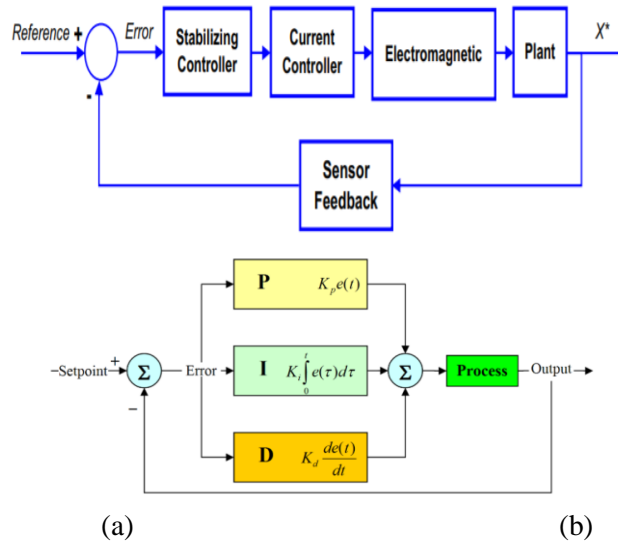
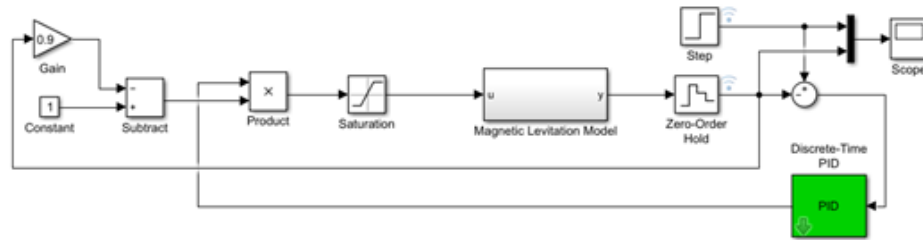


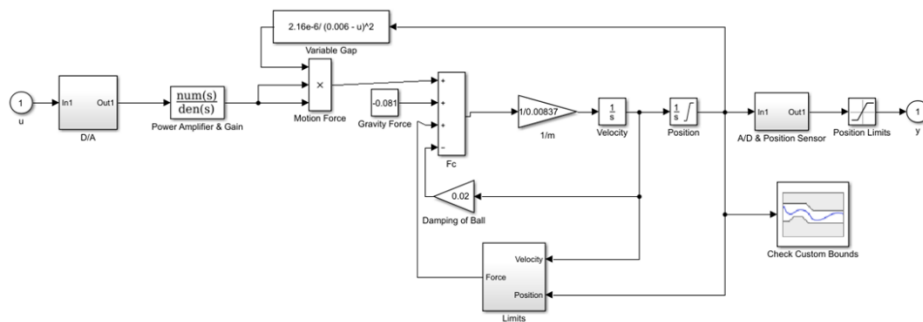
Fig. 2. Feedback and PID control mechanism of proposed maglev.

#### 4. Results and discussion

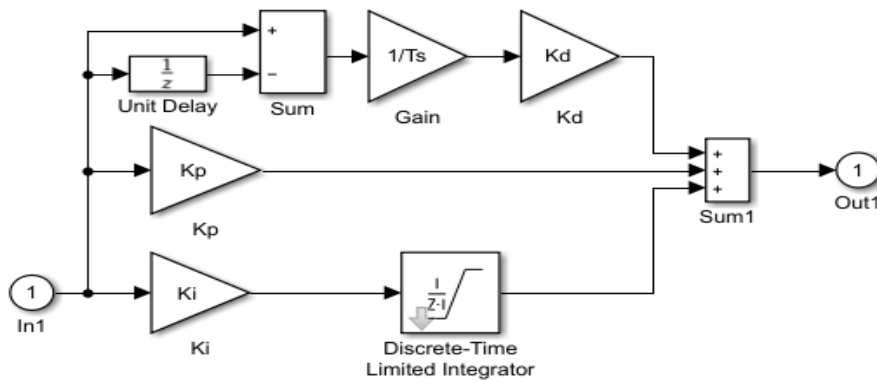
In this section, the experimental and simulation results were obtained based on different parameters and according to the proposed system design in Fig. 3(a). In this paper, three types of controllers were applied to the electromagnetic levitation prototype. The interfacing of hardware-controlled unit parts is explained in Fig. 3(b). A real-time control feature of Simulink which supports the microcontroller (SIMLAB) has been employed. Feedback control for this system is designed utilizing linear control theory. The overall architecture comprising of data acquisition hardware (SIMLAB) sensor, electromagnetic coils and real-time operating environment is shown in Fig. 3(c). The (SIMLAB) platform is a versatile, complete and low-cost real-time package with 15.2 kHz sampling rates. Moreover, (SIMLAB) is fully integrated into MATLAB and Simulink with highly intuitive usage. A conversion of displacement sensor signal to digitized value is first carried out using analog to digital (A/D) converter. The stability controller processed digitized value and send it through computer to digital to analog (D/A) port of the microcontroller. The simulation is mainly focused to simulate a Magnetic levitation system by using Proportional-Integral-Derivative Control method. The Simulation was first formulated in Simulink using its block features.



(a)



(b)

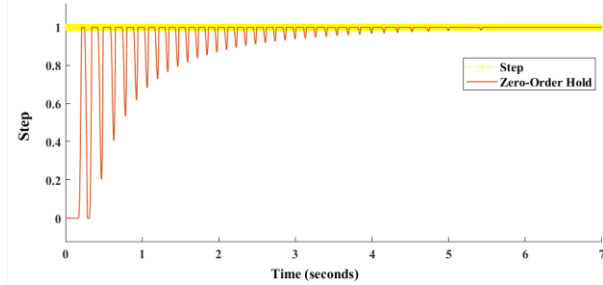


(c)

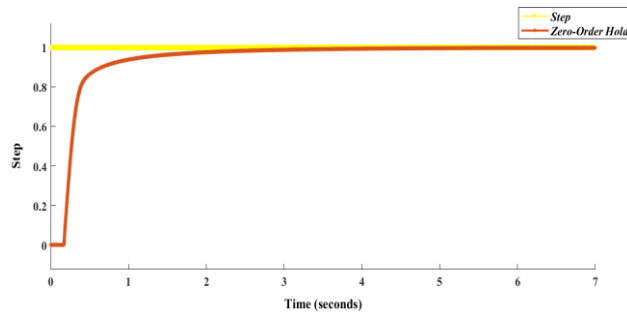
Fig. 3. Simulation modelling using MATLAB and Simulink platform (a)Whole System, (b) Detailed Mathematical Model, (c) Utilized PID model.

Microcontroller produces control current corresponding to coil magnetic field. The generated PWM value is then sent to current controller to produce corrective control current i.e., electromagnetic force. Therefore, since the load is varied and position must be maintained, then feedback control will adjust the strength of the

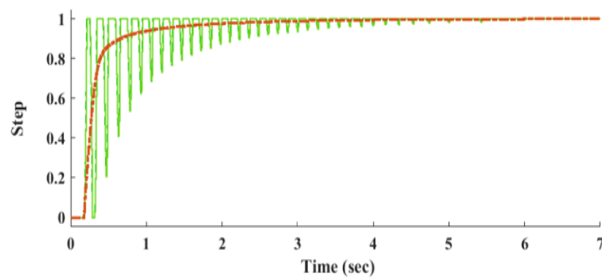
magnetic field to hold the suspended object in the desired position. The block diagram representation of overall control system is illustrated in Fig. 4 (a), where the '1' is the desired output. The simulation results of the system are shown in Fig. 4(b). From the simulation results indicating in Fig. 4(c), after applying the square wave input signal on the system and in the available of LQR controller the system performance was stable and its responds are perfect compared to PID and Lead compensation which offers less stability and slower response.



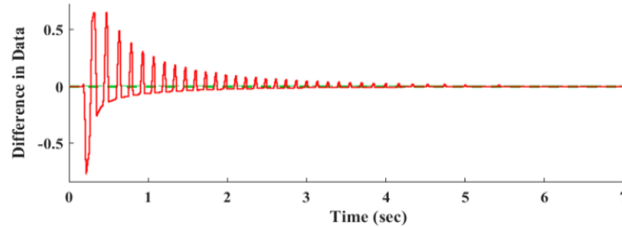
a.



b.

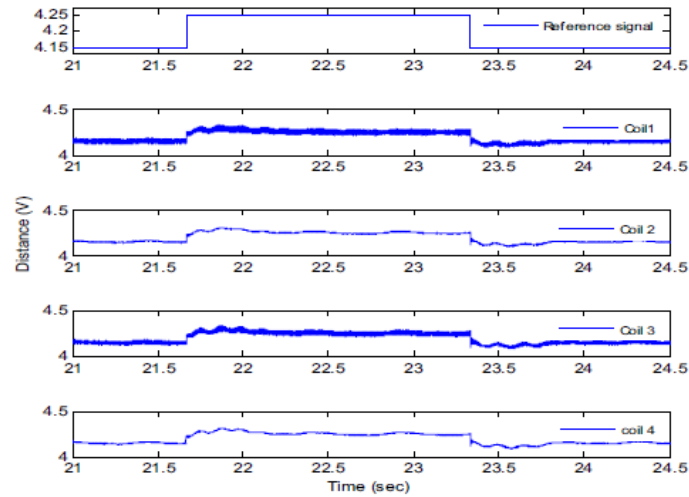


c.



d.





e.

Fig. 4. Simulated Results with comparison to referred [1] experimental validation.

Where the output signals figured at the four coils are almost identical to the reference input signal. Furthermore, The controller exhibit more robustness in performance compared with the used controllers, represented by minimum peak overshoot in the range of 0.505%, and an optimum values of setting time and Rise time of 0.102 and 0.115 respectively, which is better than PID and Lead controller [1]. Subsequent as in Fig. 4(e), the experimental results verified the simulation results. System outputs display the same behavior and trend in the system response criteria when the system was implemented with the simulation. The real-time results explained that LQR controller introduced efficient response and better stability than PID and Lead compensation under the effect of same input signal and parameters. The little difference in the results between simulation and experiment that some parameter assumption has been neglected in the simulation.

## 5. Conclusion

This paper investigates the modeling and design of a real-time magnetic-levitation (maglev) system. The control scheme for the maglev transportation system has been implemented experimentally and it was verified by the simulations. Furthermore, the suggested system was performing with three types of controllers which are LQR, PID and Lead compensation. The controller's types have been compared in term of three parameters which are peak overshoot, Rise time and settling time. The findings displayed an agreement of experimental with simulation results were obtained. Moreover, the LQR controller showed higher stability and response in comparison with classical controller types used for all the system parameters utilized. Experimentally, the LQR appeared a 14.6%, 0.199 and 0.0.64 for Peak overshoot, Setting time and Rise time respectively.

## References

- [1] Sun Jiefu, Jianning Zhu, Bihong Lu, *Research of the brake pad eccentric wear simulation of medium-low speed maglev train based on RecurDyn*, 16<sup>th</sup> International Conference on Ubiquitous Robots (UR), IEEE, 2019, p. 631-635.
- [2] Gong Junhu, *Structural form and dynamic characteristics of high-speed maglev separated track beam*, Journal of Vibration Engineering & Technologies, **10**, 6, 2022, p. 2283-2291.
- [3] Zhang Min, Cheng Yuan, Weihua Ma, Shihui Luo, *Curve negotiation performance of a newly-designed medium and low speed maglev vehicle*, Proceedings of the Institution of Mechanical Engineers, Part F: Journal of Rail and Rapid Transit, **237**, 7, 2023, p. 893-905.
- [4] Liu Jiali, Mengge Yu, Dawei Chen, Zhigang Yang, *Study on Interior Aerodynamic Noise Characteristics of the High-Speed Maglev Train in the Low Vacuum Tube*, Applied Sciences, **12**, 22, 2022, p. 11444.
- [5] He Yunfeng and Qinfen Lu, *Permanent Magnet or Additional Electromagnet Compensation Structures of End Electromagnet Module for Mid-Low Speed Maglev Train*, World Electric Vehicle Journal, **13**, 5, 2022, p. 72.
- [6] Yaghoubi Shakiba and Georgios Fainekos, *Worst-case satisfaction of stl. specifications using feedforward neural network controllers: a lagrange multipliers approach*, ACM Transactions on Embedded Computing Systems (TECS), **18**, 5s, 2019, p. 1-20.
- [7] Gao Tao, Jie Yang, Limin Jia, Yongfang Deng, Weihua Zhang, Zhenli Zhang, *Design of new energy-efficient permanent magnetic maglev vehicle suspension system*, IEEE, Access 7, 2019, p. 135917-135932.
- [8] Suganthan Ponnuthurai N. and Rakesh Katuwal, *On the origins of randomization-based feedforward neural networks*, Applied Soft Computing, **105**, 2021, p. 107239.
- [9] Frenkel Charlotte, Martin Lefebvre and David Bol, *Learning without feedback: Fixed random learning signals allow for feedforward training of deep neural networks*, Frontiers in neuroscience, **15**, 2021, p. 629892.
- [10] Zhou Ruikun, Thanin Quartz, Hans De Sterck, Jun Liu, *Neural Lyapunov control of unknown nonlinear systems with stability guarantees*, Advances in Neural Information Processing Systems, **35**, 2022, p. 29113-29125.
- [11] Chhillar Ankit and Ankur Choudhary, *Mobile robot path planning based upon updated whale optimization algorithm*, 10<sup>th</sup> International Conference on Cloud Computing, Data Science & Engineering (Confluence), IEEE, 2020, p. 684-691.
- [12] Pei Yawei, *Analysis of the Second Kinds of Edge End Effects in Medium and Low Speed Maglev Linear Motors*, The proceedings of the 16<sup>th</sup> Annual Conference of China Electrotechnical Society, Volume III, Singapore: Springer Nature Singapore, 2022, p. 35-43.
- [13] Lu Qinfen, Yanxin Li, Yunyue Ye, Z. Q. Zhu, *Investigation of forces in linear induction motor under different slip frequency for low-speed maglev application*, IEEE Transactions on energy conversion, **28**, 1, 2012, p. 145-153.
- [14] Zhu Haiyue, Chee Khiang Pang, Tat Joo Teo, *Analysis and control of a 6 DOF maglev positioning system with characteristics of end-effects and eddy current damping*, Mechatronics, **47**, 2017, p. 183-194.
- [15] Guo Xiaozhou, Bin Zhou and Jisan Lian, *A new method to reduce end effect of linear induction motor*, Journal of Modern Transportation, **20**, 2012, p. 88-92.
- [16] Wang Xiaohua, Ying Lin, Fei Ni, Diqiang Lu, *A Low-speed Maglev Speed Increasing Plan by Adopting 3000V DC Power Supply*, 12<sup>th</sup> International Symposium on Linear Drives for Industry Applications (LDIA), IEEE, 2019, p. 1-6.